

Open-Chain and Cyclic Protonated Ozone: The Ground-State Potential-Energy Hypersurface

Cynthia Meredith,[†] Geoffrey E. Quelch,* and Henry F. Schaefer, III

Contribution from the Center for Computational Quantum Chemistry, University of Georgia, Athens, Georgia 30602. Received June 18, 1990

Abstract: Theoretical studies have been performed in an attempt to elucidate the intricate potential-energy hypersurface of protonated ozone (HO_3^+). Protonation of both open-chain (C_{2v}) and cyclic (D_{3h}) forms of ozone (O_3) has been investigated. Methods used involved self-consistent-field (SCF) and coupled cluster including all single and double substitutions (CCSD) geometry optimizations utilizing a double- ζ plus polarization (DZ+P) basis. Harmonic vibrational frequencies have been predicted at the SCF level in order to characterize the stationary points obtained. In addition, single and double excitation configuration interaction (CISD) and CISD+Q single-point energies were determined for all stationary points. The global minimum for HO_3^+ was found to be a terminally attached proton on open-chain ozone in a trans arrangement, with the corresponding cis isomer 3.6 kcal mol⁻¹ higher in energy. Protonation of ozone does not preferentially stabilize the cyclic isomer relative to the open-chain form.

Introduction

The equilibrium structure and the harmonic vibrational frequencies of both the open-chain (C_{2v}) and the cyclic (D_{3h}) forms of ozone (O_3) have been a matter of considerable interest for several decades. While the experimental equilibrium geometries and frequencies of the ozone C_{2v} isomer have been well-established,^{1,2} theory has had great difficulty in accurately reproducing the geometries and frequencies simultaneously. The D_{3h} form, which was first proposed in a 1967 paper by Peyerimhoff and Buenker³ but has not yet been detected experimentally, has proven to be difficult to describe theoretically as well.

A survey of the voluminous literature⁴⁻³⁰ on O_3 confirms that this molecule indeed has been vexing to theoreticians. During the past 20 years, numerous investigators have postulated a variety of theoretical approaches to describe more precisely the diradical character of the C_{2v} isomer. In more recent years, however, attention has been focused increasingly on the geometry of the elusive D_{3h} isomer and consequently on the energy separation between the two forms.

Goddard, Dunning, Hunt, and Hay³¹ were among the first investigators to propose an innovative approach to the problem of ozone. In a persuasive 1973 paper, they asserted that their generalized valence bond (GVB) method, which combines some attributes of both the valence bond and molecular orbital (MO) methods, describes ozone more properly than does the SCF method alone. Shortly thereafter, Hay, Dunning, and Goddard³² published configuration interaction (CI) results based upon GVB wave functions for ozone evaluated at various geometries. In addition, they found that the 2^1A_1 state has 60° bond angles (D_{3h} ozone) and offered an early prediction of the energy difference between the C_{2v} and D_{3h} forms. Lucchese and Schaefer³³ subsequently combined correlated methods (CI) with a larger basis set to study the problem of the C_{2v} - D_{3h} energy separation. Their results indicate that electron correlation is more important for the C_{2v} isomer than for the D_{3h} isomer.

In 1987 Lee, Allen, and Schaefer³⁴ applied their theoretical formulation for analytic evaluation of two-configuration SCF-CI (TCSCF-CI) first derivatives to the ozone problem. Their results confirmed that a multireference wave function, due to its superior description of the diradical character of ozone, yields a structure that is much improved relative to that obtained from a single-reference description. More recently, Stanton, Bartlett, Magers, and Lipscomb³⁵ published a study of the O_3 potential energy hypersurface in which highly correlated single-reference theories (namely, many-body perturbation theory (MBPT) and the coupled cluster approach) were employed at various levels of approximation. Their paper discusses the diradical character of ozone and the levels of approximation required to achieve quantitative

agreement with experiment. Later work by Scuseria, Lee, Scheiner, and Schaefer³⁶ confirmed the observation that coupled

- (1) Hughes, R. H. *J. Chem. Phys.* **1956**, *24*, 131.
- (2) Tanaka, T.; Morino, Y. *J. Mol. Spectrosc.* **1970**, *33*, 538.
- (3) Peyerimhoff, S. D.; Buenker, R. J. *J. Chem. Phys.* **1967**, *47*, 1953.
- (4) Mulliken, R. S. *Can. J. Chem.* **1958**, *36*, 10.
- (5) Rothenberg, S.; Schaefer, H. F. *Mol. Phys.* **1971**, *21*, 317.
- (6) Yamaguchi, K. *Int. J. Quantum Chem.* **1980**, *18*, 101.
- (7) Hayes, E. F.; Siu, A. K. *Q. J. Am. Chem. Soc.* **1971**, *93*, 2090.
- (8) Wright, J. S. *Can. J. Chem.* **1973**, *51*, 139.
- (9) Blint, R. J.; Newton, M. D. *J. Chem. Phys.* **1973**, *59*, 6220.
- (10) Shih, S.; Buenker, R. J.; Peyerimhoff, S. D. *Chem. Phys. Lett.* **1974**, *28*, 463.
- (11) Hirst, D. M. *Mol. Phys.* **1976**, *31*, 1511.
- (12) Burton, P. G.; Harvey, M. D. *Nature* **1977**, *266*, 826.
- (13) Hay, P. J.; Dunning, T. H., Jr. *J. Chem. Phys.* **1977**, *67*, 2290.
- (14) Harding, L. B.; Goddard, W. A., III. *J. Chem. Phys.* **1977**, *67*, 2377.
- (15) Hiberty, P. C.; Leforestier, C. *J. Am. Chem. Soc.* **1978**, *100*, 2012.
- (16) Rodwell, W. R. *J. Am. Chem. Soc.* **1978**, *100*, 7209.
- (17) Karlström, G.; Engström, S.; Jönsson, B. *Chem. Phys. Lett.* **1978**, *57*, 390.
- (18) Laidlaw, W. G.; Trsic, M. *Chem. Phys.* **1979**, *36*, 323.
- (19) Lengsfeld, B. H., III; Schug, J. C. *Mol. Phys.* **1978**, *35*, 1113.
- (20) Burton, P. G. *J. Chem. Phys.* **1979**, *71*, 961.
- (21) Wilson, C. W., Jr.; Hopper, D. G. *J. Chem. Phys.* **1981**, *74*, 595.
- (22) Laidig, W. D.; Schaefer, H. F. *J. Chem. Phys.* **1981**, *74*, 3411.
- (23) Adler-Golden, S. M.; Langhoff, S. R.; Bauschlicher, C. W.; Carney, G. D. *J. Chem. Phys.* **1985**, *83*, 255.
- (24) Dupuis, M.; Lester, W. A., Jr. *Theor. Chim. Acta* **1987**, *71*, 255.
- (25) Rendell, A. P. L.; Bacskay, G. B.; Hush, N. S.; Handy, N. C. *J. Chem. Phys.* **1987**, *87*, 5976.
- (26) Duran, M.; Yamaguchi, Y.; Osamura, Y.; Schaefer, H. F. *J. Mol. Struct. (THEOCHEM)* **1988**, *163*, 389.
- (27) Alberts, I. L. Ph.D. Thesis, Department of Theoretical Chemistry, Cambridge University, England, 1988.
- (28) Raghavachari, K.; Trucks, G. W.; Pople, J. A.; Replogle, E. *Chem. Phys. Lett.* **1989**, *158*, 207.
- (29) Cotton, F. A.; Wilkinson, G. *Advanced Inorganic Chemistry*, 5th ed.; John Wiley & Sons: New York, 1988; pp 452-454.
- (30) Morrison, R. T.; Boyd, R. N. *Organic Chemistry*, 4th ed.; Allyn and Bacon, Inc.: Boston, 1983; pp 384-386, 450-451.
- (31) Goddard, W. A., III; Dunning, T. H., Jr.; Hunt, W. J.; Hay, P. J. *Acc. Chem. Res.* **1973**, *6*, 368.
- (32) Hay, P. J.; Dunning, T. H., Jr.; Goddard, W. A., III. *J. Chem. Phys.* **1975**, *62*, 3912.
- (33) Lucchese, R. R.; Schaefer, H. F. *J. Chem. Phys.* **1977**, *67*, 848.
- (34) Lee, T. J.; Allen, W. D.; Schaefer, H. F. *J. Chem. Phys.* **1987**, *87*, 7062.
- (35) Stanton, J. F.; Lipscomb, W. N.; Magers, D. H.; Bartlett, R. J. *J. Chem. Phys.* **1989**, *90*, 1077. Stanton, J. F.; Bartlett, R. J.; Magers, D. H.; Lipscomb, W. N. *Chem. Phys. Lett.* **1989**, *163*, 333.

[†] Charles A. Coulson Graduate Fellow.

cluster theory including all single and double substitutions (CCSD) with a DZ+P basis set reproduces the experimental equilibrium geometry and harmonic vibrational frequencies very well. However, these investigators noted that a more complete treatment of triple and quadruple excitations (as in the work of Stanton et al.³⁵) is necessary to describe many other properties of ozone with quantitative accuracy. Shortly thereafter, Lee and Scuseria³⁷ undertook such a study in which they showed that the CCSD(T) method (CCSD with perturbational inclusion of triple substitutions) coupled with large atomic natural orbital (ANO) basis sets (including *f*-type functions) would for the first time provide a quantitatively accurate description of ozone. Lee³⁸ very recently applied this method, with the addition of *g*-type functions, to the D_{3h} isomer to yield a C_{2v} - D_{3h} energy separation of 28.7 kcal mol⁻¹, establishing that the D_{3h} isomer indeed lies above the experimental dissociation limit of $\tilde{\chi}^1 A_1 O_3$.³⁹

Comparatively few studies of protonated ozone have appeared thus far. Olah, Yoneda, and Parker⁴⁰ first raised the question of the chemical significance of protonated ozone in their 1976 paper on superacid-catalyzed oxygenation of alkanes with ozone. According to Olah et al., mechanistic studies of acid-catalyzed ozonolysis are consistent with electrophilic insertion by HO_3^+ into a σ bond of the alkane. However, attempts to observe HO_3^+ directly via ¹H NMR spectroscopy were unsuccessful. Subsequent to the paper of Olah et al., two ab initio studies of HO_3^+ were published—one by Kausch and Schleyer⁴¹ and the other by Mathisen, Gropen, Skancke, and Wahlgren.⁴² Kausch and Schleyer's investigation attempted to determine the structure of HO_3^+ as well as to address the question of whether protonation might preferentially stabilize cyclic ozone enough to make it competitive with the open forms. This study, in which basis sets ranging from STO-3G to 6-31G* were employed, included both SCF and second-order Møller-Plesset perturbation (MP2) theory. While lower levels of theory (e.g., STO-3G SCF) are sometimes sufficient to locate stable potential minima, it has been established that the MP2 method yields variable results for systems with appreciable multireference character, such as ozone. For example, Kausch and Schleyer's work⁴¹ has shown that ΔE values are highly sensitive to increase in basis set size at a given level of theory as well as to improvement in the sophistication of the theoretical method within a given basis set. Mathisen et al.⁴² used larger basis sets to study HO_3^+ and related molecules at the SCF level of theory. Not surprisingly, their findings were consistent with the early work of Kausch and Schleyer. The current investigation, which is concerned primarily with protonation of both forms of ozone, improves upon these previous studies by applying more sophisticated correlated methods as well as a more extensive basis set to this problem.

Theoretical Methods

Both the C_{2v} and the D_{3h} species were protonated at various sites and each possible structure examined at the self-consistent-field (SCF) level of theory. Configuration interaction energies⁴³ were then obtained for each structure that corresponded to a stationary point. All minima on the surface were optimized at the CCSD level of theory, with CCSDT-1 (coupled cluster including single, double, and linearized triple substitutions) energies⁴⁴ evaluated at the CCSD-optimized geometries. Optimizations were performed utilizing SCF⁴⁵ and CCSD⁴⁶ analytic gradient

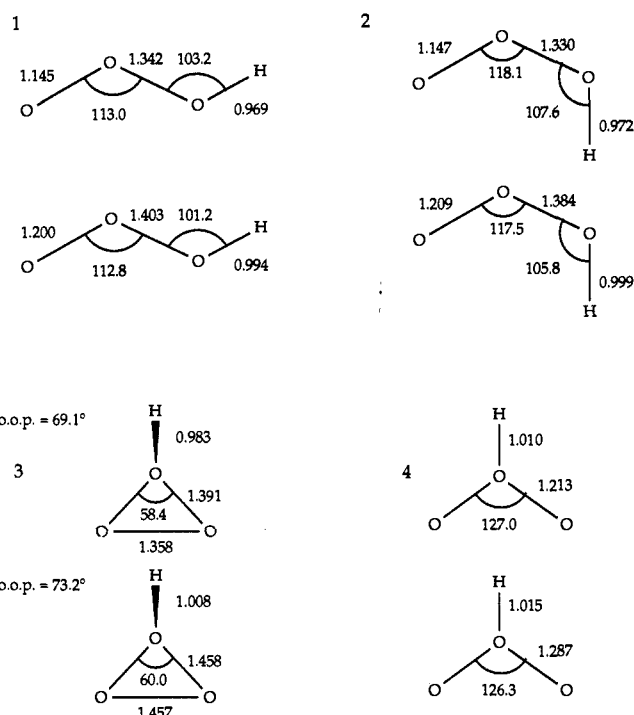


Figure 1. Geometries predicted at the DZ+P SCF (above) and CCSD (below) levels for protonated ozone (HO_3^+). All structures are minima at the SCF level of theory.

methods, with harmonic vibrational frequencies obtained from SCF analytic second derivatives.⁴⁷ In addition, the lowest energy transition state was studied at the CCSD level of theory. Its structure was optimized, and its harmonic vibrational frequencies were obtained by finite central differences of analytic gradients in internal coordinates.

The basis set used in this research was the standard double- ζ plus polarization (DZ+P) set of Huzinaga⁴⁸ and Dunning.⁴⁹ The polarization function orbital exponents chosen were $\alpha_d(O) = 0.85$ and $\alpha_p(H) = 0.75$. The DZ+P CISD wave functions in C_s symmetry in which the reflection plane is that of the molecule include 36714 configurations, whereas those in which the plane of symmetry is perpendicular to the plane of the molecule include 34531 configurations (the C_{3v} isomer, for computational reasons, was studied in C_s symmetry). For the C_{2v} structures the isomers derived from open-chain ozone include 18464 configurations, while those derived from cyclic ozone include 17872 configurations. The C_1 symmetry structure consists of 68635 configurations. The total energies given as E_{CISD+Q} are CISD energies corrected for unlinked quadruple excitations with the method of Davidson.⁵⁰

Since it has been established that the coupled cluster method reproduces C_{2v} ozone's experimental geometry and infrared frequencies reasonably well,³⁶ one might ask why CCSD optimizations were only performed for the HO_3^+ isomers representing the stable minima and the lowest energy transition state. A comparison of the CISD+Q single-point energy differences at the SCF-optimized structures of both forms of ozone and all protonated minima with the energies of the analogous CCSD-optimized structures shows that the CISD+Q and CCSD energies are nearly identical (cf. Table III). Thus it is assumed that CCSD-optimized structures of our transition states and stationary points of Hessian index two would alter the SCF-generated structures in a predictable manner—i.e., all bonds would lengthen modestly. In order to test this assumption we have optimized the structure and obtained harmonic vibrational frequencies for the transition state connecting the trans and cis isomers, which are the two lowest minima on the surface. Our results (cf. Figure 2) confirm this view.

The SCF harmonic vibrational frequencies in this study were predicted solely for the purpose of characterizing the stationary points on the

(36) Scuseria, G. E.; Lee, T. J.; Scheiner, A. C.; Schaefer, H. F. *J. Chem. Phys.* **1989**, *90*, 5635.

(37) Lee, T. J.; Scuseria, G. E. *J. Chem. Phys.* **1990**, *93*, 489.

(38) Lee, T. J. *Chem. Phys. Lett.* **1990**, *169*, 529.

(39) *Natl. Stand. Ref. Data Ser. Natl. Bur. Stand.* **1971**, *37*.

(40) Olah, G. A.; Yoneda, N.; Parker, D. G. *J. Am. Chem. Soc.* **1976**, *98*, 5261.

(41) Kausch, M.; Schleyer, P. v. R. *J. Comp. Chem.* **1980**, *1*, 94.

(42) Mathisen, K. B.; Gropen, O.; Skancke, P. N.; Wahlgren, U. *Acta Chem. Scand. A* **1983**, *37*, 817.

(43) Brooks, B. R.; Schaefer, H. F. *J. Chem. Phys.* **1979**, *70*, 5092. Saxe, P.; Fox, D. J.; Schaefer, H. F.; Handy, N. C. *J. Chem. Phys.* **1982**, *77*, 5584.

(44) Lee, Y. S.; Bartlett, R. J. *J. Chem. Phys.* **1984**, *80*, 4371. Scuseria, G. E.; Schaefer, H. F. *Chem. Phys. Lett.* **1988**, *146*, 23. Scuseria, G. E.; Schaefer, H. F. *Chem. Phys. Lett.* **1988**, *148*, 205.

(45) Pulay, P. *Modern Theoretical Chemistry*; Schaefer, H. F., Ed.; Plenum: New York, 1977; Vol. 4, pp 153-185.

(46) Scheiner, A. C.; Scuseria, G. E.; Lee, T. J.; Rice, J. E.; Schaefer, H. F. *J. Chem. Phys.* **1987**, *87*, 5361.

(47) Pople, J. A.; Krishnan, R.; Schlegel, H. B.; Binkley, J. S. *Int. J. Quantum Chem.* **1975**, *S13*, 225. Saxe, P.; Yamaguchi, Y.; Schaefer, H. F. *J. Chem. Phys.* **1982**, *77*, 5647. Osamura, Y.; Yamaguchi, Y.; Saxe, P.; Vincent, M. A.; Gaw, J. F.; Schaefer, H. F. *Chem. Phys.* **1982**, *72*, 131.

(48) Huzinaga, S. *J. Chem. Phys.* **1965**, *42*, 1293.

(49) Dunning, T. H. *J. Chem. Phys.* **1970**, *53*, 2823.

(50) Langhoff, S. R.; Davidson, E. R. *Int. J. Quantum Chem.* **1974**, *8*, 61.

Table I. Harmonic Vibrational Frequencies (cm^{-1}), Infrared Intensities (km mol^{-1}), and Assignments for the DZ+P SCF Minima of HO_3^+

	3896	445	O-H stretch
	1991	4	O-O terminal stretch
	1603	139	O-O-H deformation
	1003	32	O-O central stretch
	728	5	O-O-O deformation
	445	195	O-O-O-H torsion
	3839	276	O-H stretch
	1960	36	O-O terminal stretch
	1636	31	O-O-H deformation
	1018	96	O-O central stretch
	707	18	O-O-O deformation
	475	174	O-O-O-H torsion
	3693	535	O-H stretch
	1430	78	O-O sym stretch
	1402	60	H o.o.p.
	1204	118	H wag
	950	42	O-O-O deformation
	902	0	O-O asym stretch
	3333	562	O-H stretch
	1596	2	H wag
	1359	4	O-O sym stretch
	1294	916	O-O asym stretch
	966	149	H o.o.p.
	752	35	O-O-O deformation

potential energy hypersurface, and as such they should not be construed as attempts to achieve quantitative accuracy. An examination of the frequencies obtained in this study reveals that all of our imaginary vibrational frequencies are of sufficient magnitude that the use of correlated methods is unlikely to eliminate them entirely—indeed, the CCSD imaginary frequency obtained for isomer **13** is in fact 63% greater than the corresponding SCF frequency. Consequently we are unable to justify the enormous computational expense of generating CCSD geometries and harmonic vibrational frequencies for all first- and second-order saddle points.

All studies were performed with the PSI system of programs.⁵¹

Results

Thirteen protonated isomers, derived both from the open-chain and the cyclic forms of O_3 , are postulated for HO_3^+ . SCF geometry optimizations of these possible forms yields four stable potential minima (isomers **1–4**). The SCF geometries of all stable protonated forms of O_3 (minima), along with their CCSD-optimized structures, are shown in Figure 1, while Figure 2 depicts the SCF geometries of all transition states and higher order stationary points (CCSD values are included in parentheses for isomer **13**).

Harmonic vibrational frequencies were predicted at the SCF level of theory for all 13 isomers. These frequencies, along with their infrared intensities, are listed in Tables I and II. Also listed are CCSD values for isomer **13**. It will be noted that isomers **5**, **6**, **7**, **9**, **12**, and **13** represent transition states (one imaginary frequency) whereas isomers **8**, **10**, and **11** are stationary points of Hessian index two (two imaginary frequencies). We will refer to the latter as "hilltop" structures.

The energies of each of the protonated forms at its respective equilibrium geometry are compared with one another in Table III. In addition, this table includes the T_1 diagnostic from the CCSD optimization for each isomer.⁵² Examination of these coefficients reveals that the two lowest-energy structures (isomers **1** and **2**) have considerable multireference character. However, it is unclear whether the T_1 norm gives reliable information regarding the relative usefulness of a single reference approach for a system such as ozone with obvious multireference character. Nevertheless, the values of the T_1 norm are given in Table III for the sake of completeness.

Table II. Harmonic Vibrational Frequencies (cm^{-1}), Infrared Intensities (km mol^{-1}), and Assignments for the SCF Stationary Points of Hessian Index One and Two for HO_3^+

	2223	369	O-H sym stretch
	1543	8	O-O sym stretch
	1372	664	O-O asym stretch
	1307	174	H o.o.p.
	1115	33	O-O-O deformation
	2845i	151	O-H asym stretch
	3536	1450	O-H stretch
	1417	33	O-O sym stretch
	1168	36	O-O asym stretch
	998	17	O-O-O deformation
	624	95	H wag
	1348i	340	H o.o.p.
	3718	437	O ₁ -H stretch
	1811	427	O ₂ -O ₃ stretch
	1321	162	O ₂ -O ₁ -H deformation
	441	195	O ₁ -O ₂ stretch
	135	20	O ₂ -O ₁ -O ₃ deformation
	257i	200	O ₃ -O ₁ -O ₂ -H torsion
	2368	467	O-H sym stretch
	1363	17	O-O sym stretch
	1022	1	O-O asym stretch
	906	3	O-O-O deformation
	744i	207	H o.o.p.
	1307i	65	O-H asym stretch
	2391	535	O-H sym stretch
	1381	33	O-O sym stretch
	1277	74	O-O-O def + H o.o.p.
	918	16	O-O asym stretch
	779	52	O-O-O def - H o.o.p.
	2102i	30	O-H asym stretch
	2016	882	O-H sym stretch
	1335	59	O-O sym stretch
	955	5	O-H sym deformation
	2155i	153	O-H asym stretch
	3566	2039	O-H stretch
	1854	102	O-O term stretch
	1396	281	O-O cent stretch
	843	5	O-O-O deformation
	1524i	454	O-O-O-H torsion
	1667i	439	O-O-H deformation
	2306	806	O-H sym stretch
	1658	280	O-O exo stretch
	1159	238	O-O ring stretch
	588	104	O-O-O deformation
	168	165	o.o.p.
	2416i	114	O-H asym stretch
	3863 (3600) ^a	332	O-H stretch
	1951 (1550)	11	O-O term stretch
	1535 (1277)	75	O-O-H deformation
	970 (762)	10	O-O cent stretch
	690 (563)	10	O-O-O deformation
	425i (692i)	152	O-O-O-H torsion

^aCCSD harmonic vibrational frequencies.

The qualitative valence molecular orbitals generated from our DZ+P SCF studies for both C_{2v} and D_{3h} ozone are depicted in Figures 3 and 4, respectively.

Figure 5 and 6 summarize the potential energy surface for the protonated isomers of open-chain and cyclic ozone, respectively (CISD+Q level). Isomer **7** was omitted from these figures, as it is a partially dissociated structure and as such it is unclear whether it is more closely associated with open-chain or cyclic ozone. Isomers **8**, **10**, and **11**, which correspond to "hilltop" structures, have been omitted for the sake of clarity.

Discussion

Our study of the potential energy hypersurface of HO_3^+ indicates that it is indeed more complex than previous investigators had suspected. Kausch and Schleyer,⁴¹ employing SCF and MP2 methods, obtained variable results both for the absolute and relative energies of their HO_3^+ minima. Moreover, there was tremendous variation with basis set and method. Mathisen et al.,⁴²

(51) PSI 1.0, 1989, PSITECH Inc., Watkinsville, Georgia.

(52) Lee, T. J.; Taylor, P. R. *Int. J. Quantum Chem.* **1989**, *23*, 199. Lee, T. J.; Rice, J. E.; Scuseria, G. E.; Schaefer, H. F. *Theor. Chim. Acta* **1989**, *75*, 81.

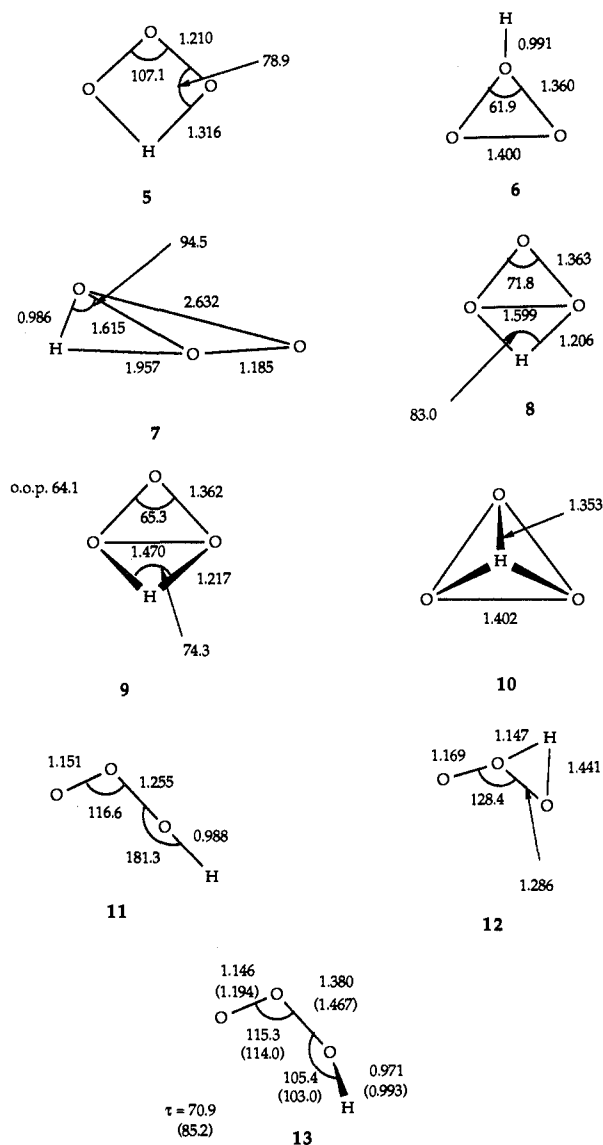


Figure 2. Geometries predicted at the DZ+P SCF level for protonated ozone (HO_3^+). All structures are stationary points of Hessian index one or two. Values in parentheses for isomer 13 are CCSD-optimized values.

utilizing the 4-31G SCF method only, also obtained results that are inconsistent with our predictions. An examination of the relative energies of our HO_3^+ isomers (Table III) demonstrates that the present results yield a potential energy surface that is qualitatively stable with respect to changes in the level of theory (a feature notably lacking in these earlier studies) due primarily to our use of polarization functions and more robust electron correlation methods. In particular it should be noted that the coupled cluster method gives reliable results for protonated ozone, as it does for the nonprotonated forms. As such, the current research adds substance to the conclusion that the DZ+P CCSD method is a reasonable "middle ground" for nontrivial problems in quantum chemistry.^{36,53}

As mentioned earlier, ozone has been notoriously difficult to describe theoretically due to its diradical character, which is seen in the form of the $1a_2$ MO as shown in Figure 3. In addition, the question of the precise C_{2v} - D_{3h} energy separation for ozone has been a subject of controversy for well over a decade. The best prediction³⁸ offered thus far, 28.7 kcal mol⁻¹, is just 3 kcal mol⁻¹ higher than that obtained from our DZ+P CISD+Q method. Study of the lowest energy protonated forms of the open-chain

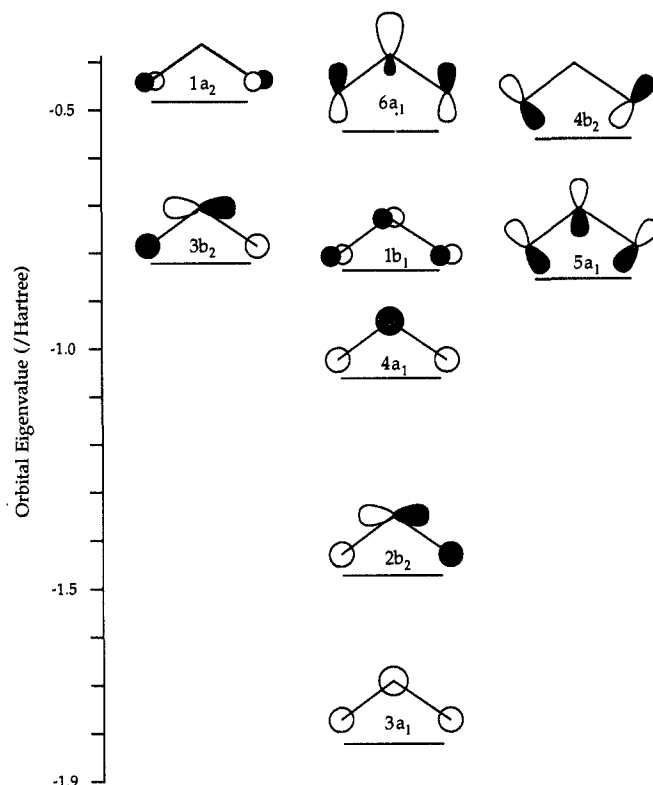


Figure 3. Qualitative molecular orbitals for the open-chain (C_{2v}) form of ozone.

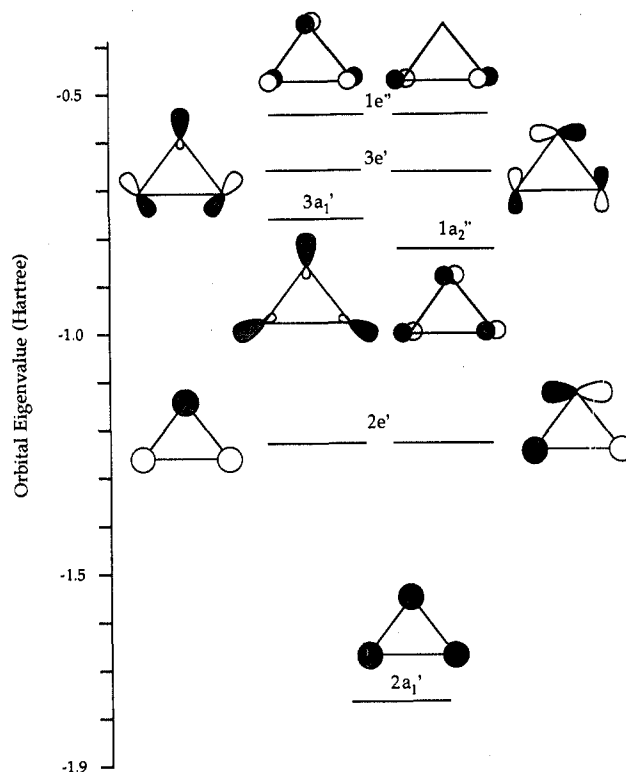


Figure 4. Qualitative molecular orbitals for the cyclic (D_{3h}) form of ozone.

(C_{2v}) and cyclic (D_{3h}) isomers demonstrates, as expected, that protonation preferentially stabilizes the open-chain form relative to the ring. The $\Delta E(\text{chain-ring})$ at the CCSD level is 23.2 kcal mol⁻¹ while the energy difference between isomers 1 and 3 is 48.1 kcal mol⁻¹.

The lowest energy HO_3^+ isomers, 1 and 2 (C_s symmetry), are derived from C_{2v} ozone, as follows. Since the $6a_1$ and $4b_2$ MOs are close in energy ($\Delta\epsilon = 14.8$ kcal mol⁻¹) and both transform

(53) Scuseria, G. E.; Hamilton, T. P.; Schaefer, H. F. *J. Chem. Phys.* **1990**, *92*, 568. Besler, B. H.; Scuseria, G. E.; Scheiner, A. C.; Schaefer, H. F. *J. Chem. Phys.* **1988**, *89*, 360.

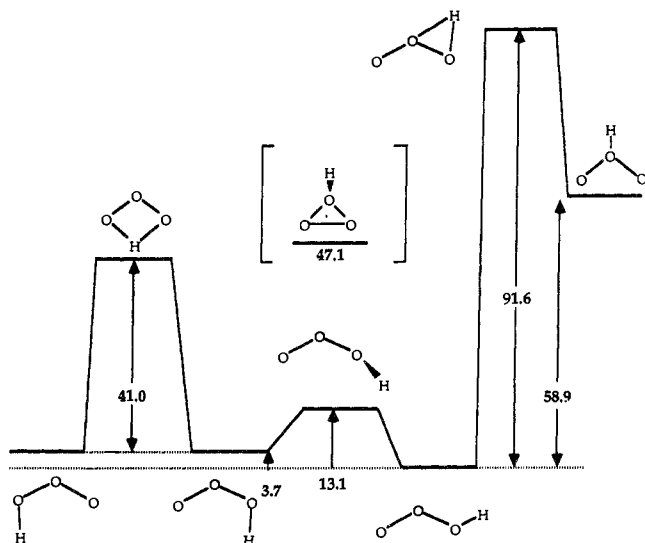


Figure 5. Potential energy hypersurface for the protonated isomers of open-chain ozone at the DZ+P CISD+Q level of theory (units in kcal mol⁻¹). Isomer 3 (the only stable minimum obtained from protonation of cyclic ozone) lies 47.1 kcal mol⁻¹ above the lowest-energy isomer of protonated open-chain ozone and is shown in brackets for purposes of comparison.

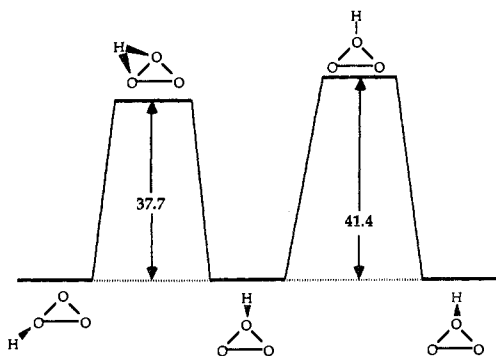


Figure 6. Potential energy hypersurface for the protonated isomers of cyclic ozone at the DZ+P CISD+Q level of theory (units in kcal mol⁻¹).

to a' orbitals in C_s symmetry (reflection plane defined in the plane of the molecule), attack of a proton on a terminal oxygen atom will allow these orbitals to mix significantly, thereby lowering the energy of the resulting a' MO. This mixing generates an orbital with electron density concentrated on the terminal oxygens only in a direction roughly perpendicular to the O-O bond axes, thus allowing for protonation in either the trans or cis mode. It is clear, then, that the orbitals of these two isomers will be closely related, which accounts for the small energy gap between them (cis 3.2 kcal mol⁻¹ higher than trans at the CCSDT-1 level). The slightly higher energy of the cis isomer is due to the fact that the hydrogen and the terminal oxygen atom are closer together in the cis than in the trans structure, and since both ends carry partial positive charges, these atoms will repel one another. This repulsion also accounts for the observation that the bond angles in the cis are $\sim 5^\circ$ larger than those in the trans isomer. Moreover, since both structures have similar bonding characteristics, deficiencies in theoretical method will tend to cancel for these isomers. This is clearly demonstrated by the ΔE values at correlated levels of theory, which differ from one another by 0.6 kcal mol⁻¹ or less (cf. Table III).

Isomer 3 (C_s symmetry with the reflection plane defined in the direction perpendicular to the ring), the only minimum generated from protonation of D_{3h} ozone, results from attachment of a proton to the a' component of the $1e''$ orbital of O_3 . This interaction decreases the antibonding character of this orbital (now the $8a'$ for HO_3^+), thereby lowering its energy and resulting in the breaking of the degeneracy of the $1e''$ orbital. Moreover, in C_s symmetry the a'' component of the $1e''$ (the SCF highest occupied

molecular orbital [HOMO]) and the $1a_2'$ (the D_{3h} SCF lowest unoccupied molecular orbital [LUMO], which is an a'' in C_s symmetry) orbitals can mix, thereby increasing the HOMO-LUMO gap of HO_3^+ relative to that of cyclic ozone. However, since the $1e''$ orbital gives rise to a' and a'' orbitals, mixing cannot occur and hence the diradical character of D_{3h} ozone is essentially retained.

Isomer 4 (C_{2v} symmetry) results from protonation on the central atom of the $6a_1$ second-highest occupied SCF MO of C_{2v} ozone. This minimum is significantly higher in energy than isomers 1 (trans) and 2 (cis) because protonation occurs only on the $6a_1$ orbital rather than on a C_s combination of C_{2v} ozone's $6a_1$ and $4b_2$ orbitals. Also, as in the case of isomers 1-3, attachment of a proton to O_3 increases the SCF HOMO-LUMO gap, thus facilitating a single-reference description of the resulting isomer. On the other hand, since the $1a_2$ SCF HOMO of ozone is unaffected by this mode of protonation, significant diradical character is retained here as well.

The geometry changes obtained with inclusion of the effects of electron correlation are as expected, i.e., a slight increase in bond lengths and a concomitant decrease in bond angles. For isomer 1 (trans), the two O-O bond lengths have increased by 0.055 (terminal) and 0.061 Å (central) whereas the O-H bond length increases from 0.969 to 0.994 Å at the CCSD level. In addition, both bond angles have decreased by about two degrees. Isomer 2 (cis) shows similar trends, with the terminal O-O length increasing by 0.062 Å, the central by 0.054 Å, and the O-H bond by 0.027 Å. The bond angles for isomer 2 (cis) have decreased as well.

The protonated ring isomer (3) shows the largest geometry changes as a result of inclusion of electron correlation. The O-O (basal) bond length, for example, has increased by 0.099 Å while the other O-O (side) bond length has increased by 0.067 Å. In fact, the O_3 ring within HO_3^+ at the CCSD level for isomer 3 is almost exactly an equilateral triangle, with bonds slightly longer than in the D_{3h} form of ozone at the CCSD level. The O-H bond length also has increased slightly and has become more nearly perpendicular to the O_3 ring. For isomer 4 the bond lengths have again increased, but less so than for isomer 3 (0.074 Å for O-O but only 0.005 Å for O-H). The O-O-O angle also has decreased slightly.

Large geometry changes also are predicted for transition state 13 upon inclusion of electron correlation (cf. Figure 2). Clearly these changes are consistent with those discussed above for the minima, namely, increases in bond length with concomitant decreases in bond angles. The dihedral angle also increases significantly, i.e., from 70.9° (SCF) to 85.2° (CCSD). This change is consistent with Hammond's postulate,⁵⁴ which states that for an endothermic reaction the transition state resembles the products more closely than the reactants.

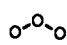
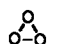
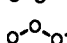

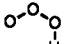
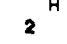
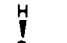
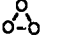
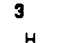
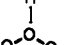
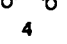
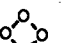
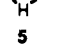
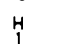
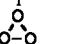
Our study reveals that protonation of the terminal oxygen of C_{2v} ozone partially destroys its diradical character, thereby improving the description of the protonated structure. This quenching of diradical character occurs as follows. In C_{2v} symmetry the SCF O_3 HOMO ($1a_2$) and LUMO ($2b_1$) cannot mix. Protonation of either the $6a_1$ or the $4b_2$ ozone MO, as mentioned earlier, reduces the molecular symmetry to C_s , thereby enabling the O_3 HOMO and LUMO (now $2a''$ and $3a''$, respectively) to mix. The mixing of these HO_3^+ MOs increases the HOMO-LUMO gap and also quenches the diradical character since there is now significant electron density at all centers.

The astute reader may have noted that, while protonation of the second- and third-highest C_{2v} ozone MOs generates stable minima at the SCF level, no such protonation of the $1a_2$ HOMO occurs. Perhaps the explanation for this is that this "HOMO" is simply an artifact of the SCF single-determinant wave function. Photoelectron ionization potential studies of ozone⁵⁵ reveal that the lowest vertical ionization gives rise to a 2A_1 state of O_3^+ with

(54) Hammond, G. S. *J. Am. Chem. Soc.* **1955**, *77*, 334.

(55) Frost, D. C.; Lee, S. T.; MacDowell, C. A. *Chem. Phys. Lett.* **1974**, *24*, 149.

Table III. Relative Energies (kcal mol⁻¹) for Isomers of HO₃⁺ at the SCF, CISD, CISD+Q, CCSD, and CCSDT-1 Levels of Theory^a

structure	ΔE_{SCF}	ΔE_{CISD}	$\Delta E_{\text{CISD+Q}}$	ΔE_{CCSD}	T_1 norm ^b	$\Delta E_{\text{CCSDT-1}}$
	163.2	157.3	157.2	158.1 ^c	0.029 ^d	148.3 ^e
	172.6	176.3	179.5	181.3	0.012	185.6
	0.0	0.0	0.0	0.0	0.048	0.0
1						
	5.0	3.8	3.7	3.6	0.046	3.2
2						
	44.6	45.0	47.1	48.1	0.016	51.4
3						
	81.0	64.1	58.9	59.6	0.025	52.5
4						
	65.2 [1]	47.7	44.7			
5						
	80.3 [1]	85.3	88.5			
6						
	79.0 [1]	<i>f</i>				
7						
	101.9 [2]	103.0	104.0			
8						
	92.9 [1]	85.6	84.8			
9						
	126.8 [2]	113.0	110.5			
10						
	60.1 [2]	57.1	57.0			
11						
	115.8 [1]	98.1	91.6			
12						
	8.5 [1]	11.8	13.1	14.9	0.034	
13						

^aAll CISD and CISD+Q values are at the appropriate SCF stationary points with the CCSDT-1 values being at the CCSD-optimized geometries except where indicated. Numbers in brackets refer to the number of imaginary frequencies at the SCF level. ^bValue described in the text. ^cResults from ref 36. ^dValue from ref 37. In this work, however, the 1s oxygen orbitals have been frozen. ^eEnergy from ref 35 at the CCSDT-1 optimized geometry. ^fThe lowest root in the CI collapses to the open-chain occupation, as described in the text.

the ²B₂ and the ²A₂ states lying successively higher in energy. This clearly violates Koopmans' theorem and as such is another indication that the MO description of ozone is poor.

Along with the four minima discussed above, numerous first- and second-order saddle points were obtained. These states were characterized through second derivative predictions and internal coordinate analyses of the resulting vibrational frequencies.

Although SCF harmonic vibrational frequencies for protonated ozone will not be quantitatively accurate, they are nevertheless useful for discerning qualitative trends, a few of which will be discussed below. A perusal of Tables I and II reveals the following. As expected, the fundamental frequencies of the trans and cis isomers of the protonated open-chain are very similar in magnitude. For example, both isomers show a high O-H stretching frequency, which is consistent with a short, strong bond. In addition, both structures give a terminal O-O stretch that is ~965

cm⁻¹ higher than that of the central O-O stretch. This finding is consistent with a relatively long central O-O bond, largely of single-bond character, and a shorter, tighter terminal O-O bond of primarily double-bond character (e.g., corresponding O-O bond lengths of the trans isomer are 1.403 and 1.200 Å, respectively, at the CCSD level). In this connection, it is useful to consider ozone as a combination of the following two resonance structures



which account for its diradical nature. Thus, it is clear that protonation of ozone on a terminal, negatively charged atom will "lock" the charge onto that end of the molecule so that the entire structure is "frozen" into one of the two degenerate resonance structures—that is, an HO₃⁺ structure in which we have an O-O

single bond and an O–O double bond, the single bond occurring at the protonated end of ozone. Experimental O–O single- and double-bond lengths for other molecules support this interpretation.⁵⁶ Moreover, it is worth noting that both the trans and cis isomers have very low torsional frequencies, which points to the possibility of a nonplanar transition state between the two forms. Our study shows that there is indeed such a transition state (isomer 13), and that the barrier to rearrangement is low ($\Delta E = 13.1$ kcal mol⁻¹ at the CISD+Q level and 14.9 kcal mol⁻¹ at the CCSD level).

It is also observed that the bridged hydrogen structures, as expected, give lower O–H stretching frequencies than those in which hydrogen is bonded to only one oxygen, with the tribridged hydrogen structure (isomer 10) giving the lowest frequency of all. Values for the infrared intensities of the minima show that all structures have at least one potentially observable band, and thus in theory experimental detection of these isomers should be possible. However, the high relative energies of the centrally protonated chain and the ring-protonated minimum suggest that the likelihood of observing these species is remote.

For the transition states and second-order saddle points, the imaginary frequencies and their assignments provide a wealth of information regarding the nature of the potential energy hypersurface. From these predictions, we were able to locate transition states connecting all minima on each part of the surface as well as the stationary points of Hessian index two and the transition states to which these lead. For example, examination of the predicted geometries and frequencies of structures 11 and 13 enabled us to identify structure 13 as the low-lying internal-rotation transition state and structure 11 as a higher-lying ($\Delta E = 57.0$ kcal mol⁻¹ at the CISD+Q level of theory) "hilltop" state between the planar trans and cis isomers (1 and 2, respectively).

As mentioned previously, harmonic vibrational frequencies were obtained for the trans–cis transition state at both the SCF and CCSD levels of theory (cf. Table II). These results differ substantially from each other, with increases in bond length tending to correlate with decreased vibrational frequencies. The imaginary frequency (assigned to the torsional internal coordinate) corresponding to conversion between the trans and cis isomers is larger in magnitude at the CCSD than at the SCF level (692i cm⁻¹ vs 425i cm⁻¹). This difference is consistent with the increased barrier height (1.8 kcal mol⁻¹) at the CCSD level of approximation.

The 1,3-dibridged open-chain (5), which has an imaginary frequency along the OH asymmetric stretching mode, is found to be a relatively high-lying transition state between the two degenerate forms of isomer 2. The branched ring isomer (6) and the out-of-plane hydrogen-bridged ring (9) similarly are transition states between the degenerate forms of isomer 3; the former structure, which has an imaginary frequency along the hydrogen out-of-plane mode, is the planar, C_{2v} transition state, whereas the latter, with an imaginary frequency along the OH asymmetric stretching mode, is the nonplanar transition state. The 1,2-dibridged open-chain (12) shows an imaginary frequency along the OH asymmetric stretching mode as well. This structure is found to be the transition state between the global minimum (1) and the higher-lying C_{2v} minimum (4).

The partially dissociated structure (7), which is omitted from Figures 5 and 6, requires some explanation. This isomer was generated by protonating D_{3h} ozone in a C_s H-bridging fashion and then optimizing the structure at the SCF level, which resulted in a structure with one imaginary frequency along an out-of-plane direction. However, SCF optimization of the resulting C₁ structure could not be performed, since in C₁ symmetry the orbital occupations of C_{2v} and D_{3h} ozone are identical and consequently the structure collapses to the lower energy open-chain configuration. For similar reasons, evaluation of the CISD energy of the ring state of isomer 7 at the C_s SCF geometry was not possible.

A closer look at this structure indicates, however, that it actually is dissociating into O₂ and OH⁺. The Mulliken charge distri-

butions for this structure confirm that most of the positive charge is localized on the hydrogen atom and the oxygen atom that is nearest to it ($r_{\text{O-H}} = 0.986$ Å). Experimental heat of formation data,⁵⁷ which show that dissociation of HO₃⁺ into O₂ + OH⁺ is energetically favored over dissociation into O₃ + H⁺ by ≈ 90 kcal mol⁻¹, support this interpretation.

As mentioned earlier, there are three stationary points of Hessian index two on the HO₃⁺ surface corresponding to isomers 8, 10, and 11. The dibridged ring (8) has imaginary frequencies along the OH asymmetric stretch and the hydrogen out-of-plane directions. If one follows each of these modes, it is found that they give rise to the transition structures 6 and 9, respectively, both of which, as noted above, collapse to the ring-protonated minimum (3). Protonation of cyclic ozone to give a C_{3v} structure results in isomer 10, which possesses a degenerate imaginary frequency along the OH asymmetric stretching mode. This structure appears to be a "hilltop" state (22.0 kcal mol⁻¹ above the branched ring (6) at the CISD+Q level) between degenerate forms of isomer 3. Structure 11, as noted previously, is a "hilltop" state between isomers 1 and 2 (12.3 kcal mol⁻¹ above the 1,3-dibridged open-chain (5) at the CISD+Q level), with the two imaginary frequencies being the out-of-plane torsion leading to the trans–cis internal rotation transition state and the OOH deformation leading to the trans global minimum (1).

Concluding Remarks

Since ozone is isoelectronic with nitrosyl fluoride (FNO) and nitrogen hypofluorite (FON) and protonation of the latter two species has been studied recently,⁵⁸ a comparison may be of interest. If we first consider FNO, we note that the trans–cis energy difference of oxygen-protonated HFNO⁺ is similar to that of trans and cis HO₃⁺ isomers (2.7 vs 3.7 kcal mol⁻¹, respectively, at the CISD+Q level). This is to be expected, since both parent structures possess terminally bonded oxygen atoms. Non-C_{2v} protonation of O₃ is more favored than protonation of FNO since the former structure, due to its diradical character, has more to gain energetically from the attachment of a proton. For FNO, protonation at the nitrogen leads to an almost identical protonation energy as compared to oxygen protonation. However, this has no comparative analogue in O₃, where central protonation is considerably less favored than at the terminal position.

Protonation at the central atom in O₃ can be compared to oxygen protonation of the FON isomer. The former protonation energy is 58.9 and the latter 82.4 kcal mol⁻¹ at the CISD+Q level.

Further comparison of ozone protonation with that of FNO and FON reveals that there are far more isomers of HO₃⁺ than of (FNO)H⁺ and (FON)H⁺ combined. One obvious reason for this is that FNO and FON are of C_v symmetry while O₃ is of C_{2v} symmetry. Moreover, since the HOMOs of FNO and FON are in-plane (i.e., 10a' in both cases), protonation of these species will yield only planar C_s isomers whereas protonation of O₃'s higher-energy valence orbitals generates numerous in-plane and out-of-plane isomers. Thus, since there are several HO₃⁺ isomers for which no protonated FNO or FON analogues exist, we will examine only the analogous isomers of HO₃⁺ and F(NO)H⁺.

For open-chain ozone, as well as for FNO and FON, protonation of the central atom generates a stable minimum. In the case of (FNO)H⁺ this nitrogen-protonated structure is the global minimum, whereas for (FON)H⁺ and HO₃⁺, lower energy structures are obtained by protonation of terminal atoms. In addition, protonation of FNO on either the nitrogen or the oxygen atom generates a stabilization of some 128–135 kcal mol⁻¹ (CISD+Q), whereas the various modes of protonation of FON and O₃ yield a wide range of stabilization energies.

In addition to elucidating the possible structures of the species HO₃⁺ (the existence of which was postulated by Olah et al.⁴⁰), the present research also attempts to answer the question of whether protonation of O₃ might preferentially stabilize the cyclic

(57) *CRC Handbook of Chemistry and Physics*, 65th ed.; Weast, R. C., Ed.; CRC Press, Inc.: Boca Raton, FL, 1984.

(58) Meredith, C.; Davy, R. D.; Schaefer, H. F. *J. Chem. Phys.* **1990**, *93*, 1215.

(56) Huheey, J. E. *Inorganic Chemistry: Principles of Structure and Reactivity*; Harper & Row: New York, 1972; p 701.

isomer relative to the open-chain form. Our results indicate that this does not happen; on the contrary, we found that the ΔE between the lowest-energy isomers of the protonated open-chain and the protonated ring is even greater than the separation between C_{2v} and D_{3h} ozone (48.1 vs 23.2 kcal mol⁻¹ at the CCSD level of theory).

The best value for the protonation energy for open-chain ozone in this work is 148 kcal mol⁻¹ (CCSDT-1 energy at the CCSD geometry), to be contrasted with the value of 124 kcal mol⁻¹ proffered by the early work of Kausch and Schleyer.⁴¹ Extensive

search of the experimental literature has failed to reveal a value for the protonation energy of ozone.

Acknowledgment. This research was supported by the U.S. Department of Energy, Office of Basic Energy Sciences, Division of Chemical Sciences, Fundamental Interactions Branch, Grant DE-FG09-87ER13811. We thank Dr. Brenda Thies Colegrove for numerous discussions and pertinent suggestions, Dr. Leo Radom for helpful correspondence, and an anonymous referee for additional suggestions.

Molecular Conformation of Nonionic Surfactants in the Solid State. A Raman Spectroscopic Study of a Homologous Series of α -*n*-Alkyl- ω -hydroxyoligo(oxyethylene)s

Hiroatsu Matsuura,^{*,†,‡} Koichi Fukuhara,[†] Sei Masatoki,[†] and Masaaki Sakakibara[§]

Contribution from the Department of Chemistry, Faculty of Science, Hiroshima University, Higashisenda-machi, Naka-ku, Hiroshima 730, Japan, and the Faculty of General Education, Tottori University, Koyama-cho Minami, Tottori 680, Japan. Received July 27, 1990

Abstract: The molecular conformation of a homologous series of nonionic surfactants, α -*n*-alkyl- ω -hydroxyoligo(oxyethylene)s $\text{CH}_3(\text{CH}_2)_{n-1}(\text{OCH}_2\text{CH}_2)_m\text{OH}$ (C_nE_m) was comprehensively investigated, as the conformational properties are fundamentals of structural and functional aspects of the surfactant systems. Raman spectra of 48 C_nE_m compounds with $n = 1-7, 9-11$, and $13-16$, and $m = 1-5$ and 7 were measured in the crystalline solid state, and their molecular conformations were determined by a systematic analysis of the spectra. The present results, amalgamated with the previous results for 23 other C_nE_m homologues, show that the molecular conformation of the consecutive C_nE_m surfactants with $n = 1-16$ and $m = 1-8$ depends not only on the oxyethylene chain length but also on the alkyl chain length and that there exist at least six distinctive conformational forms. For the compounds with $n \leq 4$, the conformation is basically helical with the predominating oxyethylene chain which intrinsically favors the helical structure. For $n \geq 5$, the molecular conformation greatly depends on the oxyethylene chain length; as the number of oxyethylene units increases, the conformation changes from a highly extended form to a helical/extended diblock form. This conformational transition takes place at $m = 3-4$. Being coincident with this transition point, C_8E_3 , $C_{12}E_3$, and $C_{16}E_3$ crystallize into either the extended form or the diblock form depending on the solidification conditions. The conformational behavior of the C_nE_m compounds is elucidated by a conformational competition between the alkyl and oxyethylene chains whose conformational characters are distinct from each other. The reported thermodynamic quantities of the C_nE_m surfactants are indicative of strong correlations with the conformational behavior of these homologous compounds. The classical model of the meander conformation of the oxyethylene chain is unlikely to exist.

Amphiphilic substances such as surfactants and lipids possess in the same molecule two different types of chemical groups, a hydrophilic group and a hydrophobic group. When these substances are in a medium, some specific interactions are expected to occur between the amphiphilic molecules and the solvent molecules as well as between the amphiphilic molecules and between the solvent molecules. The interactions involved are composed basically of hydrophilic and hydrophobic interactions.^{1,2} These interactions are essentially of solvation type and are thereby likely to depend specifically on the structure of the amphiphiles and the solvent molecules. The dual nature of the amphiphilic substances is responsible for these interactions and consequently for the specific surface activity and biological functions.^{3,4} These properties of the amphiphiles are thus greatly dependent on the structural aspects of the system. Surfactant and lipid molecules associate, in fact, into a variety of structures in aqueous or non-aqueous solutions. In these systems, conformational properties of the hydrophobic and hydrophilic portions of the amphiphilic molecules are closely related to the geometry of diverse aggregates organized in various macroscopic phases.^{5,6} Structural studies

of the amphiphilic substances are thus highly challenging in that the knowledge obtained will be eventually correlated with the mechanism of the specific interactions and the functions involved in the biological systems. In spite of this fundamental importance, however, only limited knowledge of the structural problems has in fact been available.

For the purpose of gaining an insight into the structural aspects of amphiphilic systems, we have been working on conformational analyses of fundamental amphiphilic molecules. The substances we have adopted are a series of nonionic surfactants: α -alkyl- ω -hydroxyoligo(oxyethylene)s $\text{R}(\text{OCH}_2\text{CH}_2)_m\text{OH}$ ⁷⁻⁹ and α -al-

(1) Tanford, C. *The Hydrophobic Effect: Formation of Micelles and Biological Membranes*, 2nd ed.; Wiley: New York, 1980.

(2) Israelachvili, J. N. *Intermolecular and Surface Forces: With Applications to Colloidal and Biological Systems*; Academic Press: London, 1985.

(3) Fendler, J. H. *Membrane Mimetic Chemistry: Characterizations and Applications of Micelles, Microemulsions, Monolayers, Bilayers, Vesicles, Host-Guest Systems, and Polyions*; Wiley: New York, 1982.

(4) Attwood, D.; Florence, A. T. *Surfactant Systems: Their Chemistry, Pharmacy and Biology*; Chapman and Hall: London, 1983.

(5) Degiorgio, V.; Corti, M., Eds. *Physics of Amphiphiles: Micelles, Vesicles and Microemulsions*; North-Holland: Amsterdam, 1985.

(6) Ben-Shaul, A.; Gelbart, W. M. *Annu. Rev. Phys. Chem.* **1985**, *36*, 179-211.

(7) Matsuura, H.; Fukuhara, K. *Chem. Lett.* **1984**, 933-936.

(8) Matsuura, H.; Fukuhara, K. *J. Phys. Chem.* **1986**, *90*, 3057-3059.

(9) Matsuura, H.; Fukuhara, K. *J. Phys. Chem.* **1987**, *91*, 6139-6148.

[†]Hiroshima University.

[‡]Address after October 1991: Department of Chemistry, Faculty of Science, Hiroshima University, Kagamiyama, Higashi-Hiroshima 724, Japan.

[§]Tottori University.